AJNR

MR cisternography: initial experience in 41 cases.

T el Gammal and B S Brooks

AJNR Am J Neuroradiol 1994, 15 (9) 1647-1656
http://www.ajnr.org/content/15/9/1647

MR Cisternography: Initial Experience in 41 Cases

Taher El Gammal and Betty Sue Brooks

PURPOSE: To present our initial experience with MR cisternography, an application of fast spin-echo MR with fat suppression, and compare it with routine MR cranial studies in the evaluation of the subarachnoid cisterns and their contents. **METHODS:** MR cisternography is a heavily T2-weighted fast spin-echo technique with high spatial resolution; it uses fat suppression and video reversal of the images. A small number of individual sections (two to four) are compressed into a composite image by a maximum-intensity projection algorithm, providing better depiction of anatomy in three dimensions. MR cisternography enhances the signal intensity of the cerebrospinal fluid (CSF) with suppression and subtraction of the background. A total of 41 patients were examined during a period of 6 months. MR cisternography was performed as an additional one (n = 31) or two (n = 10) sequences after conventional MR study. **RESULTS:** Twenty-one cases of disease were examined by MR cisternography, including 8 neoplasms, 4 CSF fistulas, and 3 large intracranial aneurysms. MR cisternography provided information unavailable by conventional MR studies in 17 cases. These included visualization of fistulous tracks in patients with CSF rhinorrhea, origin of a large suprasellar aneurysm, an additional loculus of a posterior fossa aneurysm and its relation to surrounding structures, and proper location of three tumors (intraaxial versus extraaxial). Clear depiction of the pituitary gland separate from the cavernous sinus was noted in 60% of the cases, and a new observation of a CSF sleeve around the third nerve in the posterior cavernous sinus was made in 85% of the cases. **CONCLUSION:** MR cisternography is superior to conventional MR studies in depicting anatomic structures within the subarachnoid spaces. This technique is recommended in the evaluation of cranial CSF fistulas and suprasellar and posterior fossa masses and in diagnosis of intraaxial versus extraaxial location of intracranial tumors.

Index terms: Cisternography; Magnetic resonance, comparative studies; Magnetic resonance, technique; Subarachnoid cisterns

AJNR Am J Neuroradiol 15:1647–1656, Oct 1994

Positive-contrast cisternography, an invasive technique, was used in the past to depict normal and abnormal images of the subarachnoid spaces and their contents in the cranial cavity and at the craniovertebral junction. The images were enhanced with the use of polytomography (1) and magnification and subtraction techniques (2–4). These studies were found useful to delineate tonsillar herniation (1), small tumors (3, 4), and large posterior fossa aneurysms (5).

Computed tomographic (CT) cisternography after intrathecal contrast injection has been used to evaluate cerebrospinal fluid (CSF) leaks from the cranial cavity (6) and in the evaluation of posterior fossa normal anatomy (7), but with magnetic resonance (MR) the need for these invasive procedures is greatly diminished. Recently fast spin-echo MR sequences have provided heavily T2-weighted images of the cranial cavity with excellent depiction of the subarachnoid spaces and their contents.

We report an MR technique, MR cisternography, which greatly enhances the details of the

Received September 28, 1993; accepted after revision January 24, 1994.

From the Department of Radiology, University of Alabama at Birmingham.

Address reprint requests to Taher El Gammal, MD, Department of Radiology, University of Alabama at Birmingham, 619 S 19th St, Birmingham, AL 35233-6830.

AJNR 15:1647–1656, Oct 1994 0195-6108/94/1509–1647

anatomic structures within the subarachnoid spaces of the brain and the craniovertebral junction, and present our initial experience in 41 cases. The technique is essentially an extension of the application of MR myelography (8) (El Gammal T, Brooks BS, Freedy M, Magnetic Resonance Myelography: Initial Experience in 80 Cases, presented at the 31st Annual Meeting of the American Society of Neuroradiology, Vancouver, Canada, May 1993) into the cranial cavity and and the craniovertebral junction.

Subjects and Methods

We examined 41 patients over a period of 6 months starting in February 1993. They were 24 male and 17 female patients ranging in age from 4 to 82 years with a mean age of 45.9 years. The patients were selected in a random fashion. Volunteers and patients with normal MR findings were included at the beginning of the study. Later, patients with suspected disease in the parasellar regions and in the posterior fossae were included. MR cisternography was not attempted on uncooperative patients.

All scans were performed on a 1.5-T Signa unit with 5× software using a standard head coil. In two cases a spine

MR cisternography findings in patients with disease (n = 21)

Cases	MR Cisternography Findings
Cranial CSF fistula (n = 4)	
1 Anterior fossa (Fig 1)[a]	Fistula track into right ethmoid sinus was only demonstrated by MR cisternography
3 Petrous bone and posterior fossa[a]	Fistula communication between left temporal horn parencephalic cyst and middle ear was only seen by MR cisternography in one patient
	Two cases of postoperative rhinorrhea, in one no fistula seen by MR cisternography, in the other a possible communication between middle fossa and petrous bone was not confirmed by surgery
Parasellar and orbit (n = 8)	
2 Pituitary adenomas	
Hemorrhagic	Showed high-signal tumor
Postoperative	Chiasmal deformity not clearly seen on conventional MR
2 Suprasellar aneurysms (Fig 5)[a] (both large)	Aneurysm origin only seen on MR cisternography; other case, wide neck and dolichoectasia only seen on MR cisternography
2 Suprasellar tumors[a]	
Craniopharyngioma[a]	Displaced chiasm only seen on MR cisternography
Subfrontal glioma[a]	Intraaxial location seen on MR cisternography and unclear on conventional MR
2 Optic nerve injury	In both cases conventional MR failed to show normal optic nerves seen on MR cisternography
With intraconal hemorrhage (trauma)[a]	
With scar from previous granuloma (Fig 2)[a] (local anesthesia)	
Posterior fossa (n = 8)	
2 Basilar aneurysms	Relation to brain stem and cranial nerves and depiction of a second loculus; these findings were not clear on conventional MR
Anterior inferior cerebellar artery (large) (Fig 7)[a]	
Anterior inferior cerebellar artery origin (small fusiform)[a]	Not seen on conventional MR and seen on MR cisternography only
1 Intracanalicular acoustic neurinoma	Shown by both composite MR cisternography and enhanced conventional MR
2 Meningiomas	
Tentorial[a]	MR cisternography showed normal tentorium; conventional MR could not rule out tumor invasion
Posterior[a]	Extraaxial location by MR cisternography, indeterminate on conventional MR
2 Intrinsic lesions	
Quadrigeminal plate glioma[a]	Shown by MR cisternography and conventional MR
Cavernous angioma of fourth ventricle[a]	Perilesional high signal seen only on MR cisternography, most likely caused by gliosis.
1 Mild Chiari II malformation	Shown by MR cisternography and conventional MR
Cerebral hemispheres (n = 1)	
Renal cell carcinoma with two supratentorial masses (Fig 8)[a]	Inferior mass shown to be extraaxial (meningioma); MR cisternography showed CSF around tumor bed, and conventional MR showed hyperostosis; superior mass shown to be intraaxial by MR cisternography, and conventional MR was inconclusive

[a] MR cisternography provided additional information (n = 17).

Fig 1. Posttraumatic recurrent CSF leak with meningitis.

A, Coronal and *B*, sagittal MR cisternography show the high signal of abnormal gyrus rectus and CSF herniating into the right anterior ethmoid sinus (*arrows* on *right*). In *A*, note the linear high signal in the left anterior ethmoid (*left arrow*). A preoperative diagnosis of fistula on the left was not made.

C, Coronal CT cisternogram shows a defect in the roof of the right anterior ethmoid sinus (*arrow*), opaque ethmoid sinuses, and no fistulous track. Only a very small amount of contrast media reached the anterior fossa probably because of posttraumatic adhesions.

phased-array coil was used to evaluate the craniovertebral junction. The MR cisternography was performed as one or two sequences (coronal and/or sagittal) after the conventional MR brain studies. The conventional MR studies included fast spin-echo axial sequences. In four patients coronal fast spin-echo sequences were performed as well.

MR cisternography, a fast spin-echo sequence with fat suppression, used an echo train length of 16, a 16-cm field of view with no phase-wrap option, 3-mm-thick sections, 10 000/200/4 (repetition time [TR]/echo time/excitations), and a 512 × 192 matrix. A total of 16 images were obtained in 8 minutes. Image video reversal was used in all the MR cisternography studies.

Twenty-seven cases had coronal studies; 4 had sagittal studies only, and 10 had both coronal and sagittal images. A small number of images were compressed into composite images using a maximum intensity projection algorithm. The number of sections used was usually two to four with a maximum of eight. If more sections are used in the composite image this will result in a complex distorted image.

The image quality of the cisternograms was subjectively rated as poor, average, good, or very good. Comparison of MR cisternography with conventional MR studies was done by one unblinded observer.

Results

Thirteen cases were normal, and seven cases showed only atrophy without other abnormalities. Findings of disease were noted in 21 cases (Table). As shown in the Table, MR cisternography was superior to conventional MR examinations, which were only axial fast spin-echo in the majority of cases. MR cisternography provided valuable additional information in 17 of 21 cases with pathologic changes. In some of these cases MR cisternography also proved superior to other neuroradiologic procedures. Specifically, MR cisternography was better than catheter angiography in locating the origin of one suprasellar aneurysm and in depicting an additional aneurysm loculus of an anterior inferior cerebellar artery aneurysm. MR cisternography was superior to CT cisternography in the diagnosis of CSF fistulas (Fig 1). In 35 cases, image quality of the MR cisternography studies was rated as very good, in five cases as good, and in one case as average.

Discussion

MR cisternography, a fast spin-echo heavily weighted T2 sequence with fat suppression, provides detailed anatomic information of the subarachnoid cisterns, their contents, and adjacent structures by virtue of its ability to increase the signal intensity of the CSF and to suppress the background. MR cisternography depicts the cranial nerves with anatomic detail unequaled by any other imaging technique. Because the outer walls of blood vessels are outlined, a representative detailed "extraluminal" angiogram is also provided. MR cisternography has nonin-

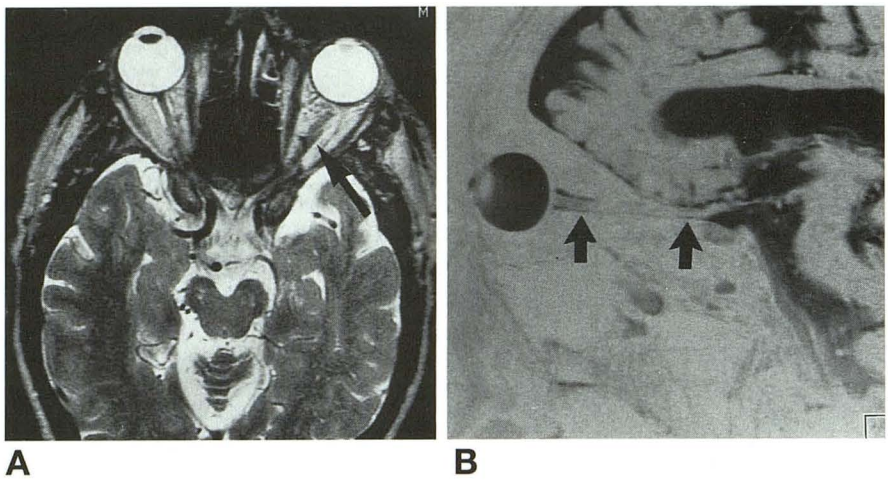

Fig 2. Left optic nerve injury after local anesthesia to the left orbit in a patient who developed diminished visual activity.

A, Transaxial MR (6500/85) shows apparent enlargement of the left optic nerve (*arrow*).

B, Oblique sagittal (composite MR cisternography) image shows the normal left optic nerve in its entire course (*arrows*). In the orbit, the nerve is surrounded by a narrow CSF sleeve compressed by a postgranuloma scar. Coronal MR cisternography failed to outline the optic nerve in the left orbit because of the compressing scar.

vasively reemphasized the importance of extraparenchymal imaging.

In this study, a long TR of 10 000 milliseconds was used in all 41 cases. We agree with Krudy (8) that an increase of the TR to more than 5000 milliseconds would not add to the scan quality. This long TR was used mainly to include 16 contiguous 3-mm-thick sections sufficient to cover a large area such as the posterior fossa. For evaluation of a limited area such as the sellar region, a TR of 5000 milliseconds is now being used, and the exam is accomplished in only 4 minutes.

Unlike MR myelography, only a few individual sections need to be compressed to obtain the needed information in MR cisternography. A composite image of all individual sections will provide a complex and nonmeaningful image. The compressed or composite images provide useful information, although some loss of detail occurs, especially if more than three sections are used. Composite images are useful in detection of fistulous tracks in patients with CSF rhinorrhea, especially when the track is irregular and tortuous. Composite images are essential in the evaluation of the internal auditory recess. A defect seen on an individual section should be confirmed by a composite image. Apparent defects can occur in individual sections because of partial volume effect of adjacent bone and/or narrow internal auditory canals. Composite images are also useful in the evaluation of the optic nerve along its entire angular course (Fig 2). Composite images were also useful in the evaluation of various mass lesions in the subarachnoid space.

Most of the conventional MR studies included gadolinium enhancement. Ideally, we should have compared MR cisternography with coronal fast spin-echo MR with high spatial resolution. In this series only four patients had coronal fast spin-echo MR studies, but MR cisternography provided better anatomic information in all four cases.

We reviewed an earlier series (n = 34) of normal MR studies of the pituitary region using coronal fast spin-echo high-resolution scans (6500/108/4 and 512 × 256 matrix or 6500/108/2 and 512 × 384 matrix). We found that 23.5% of cases (n = 8) showed good definition of the pituitary glands, clearly separate from the surrounding structures. We also found that in 30% of cases (n = 10), the CSF sleeves of the third cranial nerves in the posterior cavernous sinuses were clearly seen. In the present series the normal pituitary regions were included in 20 MR cisternography scans. In 60% of these cases (n = 12), the pituitary glands were clearly delineated separate from the adjacent cavernous sinuses by linear high signal probably caused by venous plexus (Fig 3). We also found that 85% of cases (n = 17) depicted the third-nerve CSF sleeves in the posterior cavernous sinuses (Fig 4). The higher percentage of depiction of these anatomic findings by MR cisternography suggests its superiority over conventional fast spin-echo, because associated pulsation artifacts degrade the anatomic details in the sellar regions on the conventional studies. These are greatly eliminated in MR cisternography by background suppression (Figs 3 and 4).

CSF Fistula

In two patients with delayed recurrent posttraumatic CSF leaks, MR cisternography in one

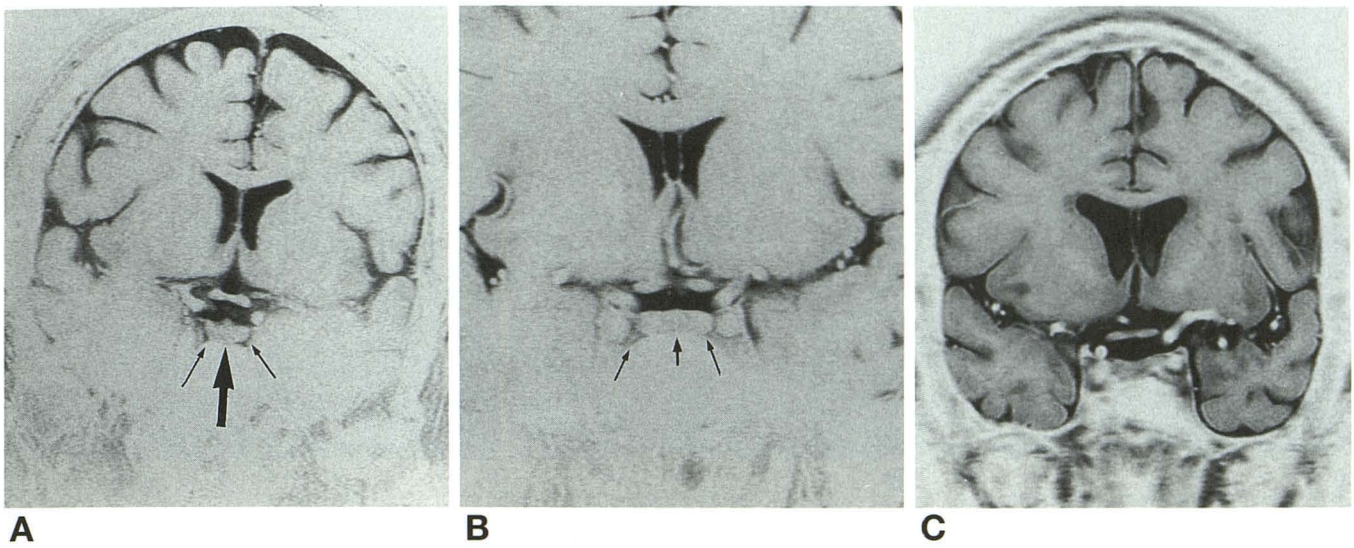

Fig 3. Normal pituitary gland is well depicted by MR cisternography but not by conventional MR.
A and *B*, MR cisternography shows clearly defined pituitary glands in two patients probably by periglandular venous plexus (*arrows*).
C, In another patient, fast spin-echo coronal (6500/108/4), 512 × 256 matrix, video reversal image. Note the distorted sellar anatomy by pulsation artifacts.

patient demonstrated a CSF track from a left temporal horn communicating porencephalic cyst into the left middle ear cavity. At surgery the fistulous communication was confirmed. The other patient had herniation of a portion of porencephalic right gyrus rectus and CSF into the right anterior ethmoid sinus (Fig 1). A linear high signal was also noted in the left anterior ethmoid sinus but was not seen continuously with the cranial CSF. The right fistula was confirmed at surgery; however, there was also another fistula extending into the left ethmoid sinus that was not diagnosed with MR cisternography. Although MR cisternography had a false-negative result on the left, we maintain that the high signal extending outside the cranial cavity should be continuous with the remainder of the CSF for a definitive diagnosis to be made. Neither CT cisternography nor conventional MR could reveal the fistula communication in either case. MR cisternography accurately depicted the fistulous tracks in these patients. It is noninvasive and cost effective, and we recommend it in the evaluation of patients suspected to have cranial CSF fistulas.

Parasellar Region and Orbit

The detailed anatomic information by MR cisternography provided an important preoperative finding in a patient with suprasellar cranio-

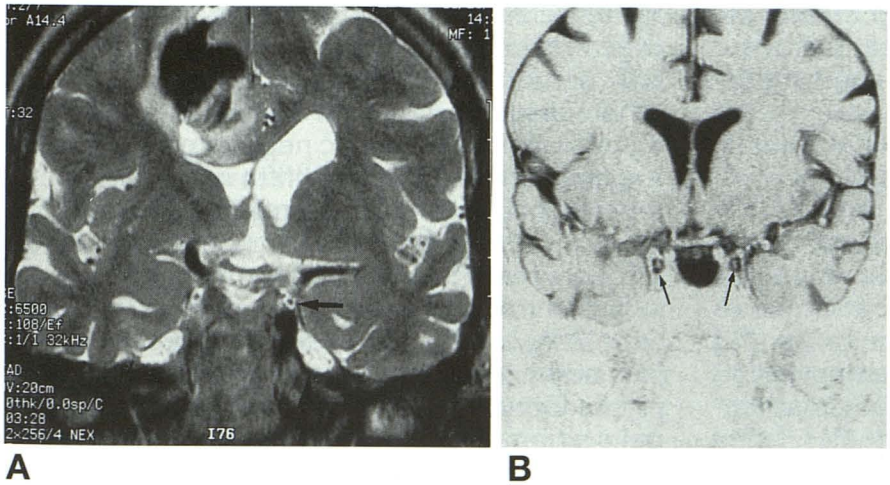

Fig 4. Normal CSF sleeve around third nerve in the posterior cavernous sinus.
A, Fast spin-echo (6500/108) in a case with cerebral hemorrhage. The third nerve within the CSF sleeve is well seen on the fast spin-echo image (*arrow*). Note, however, the lack of detail in the pituitary region caused by pulsation artifacts.
B, Coronal MR cisternography in another patient shows the CSF sleeve around the third nerve in the posterior cavernous sinus (*arrows*).

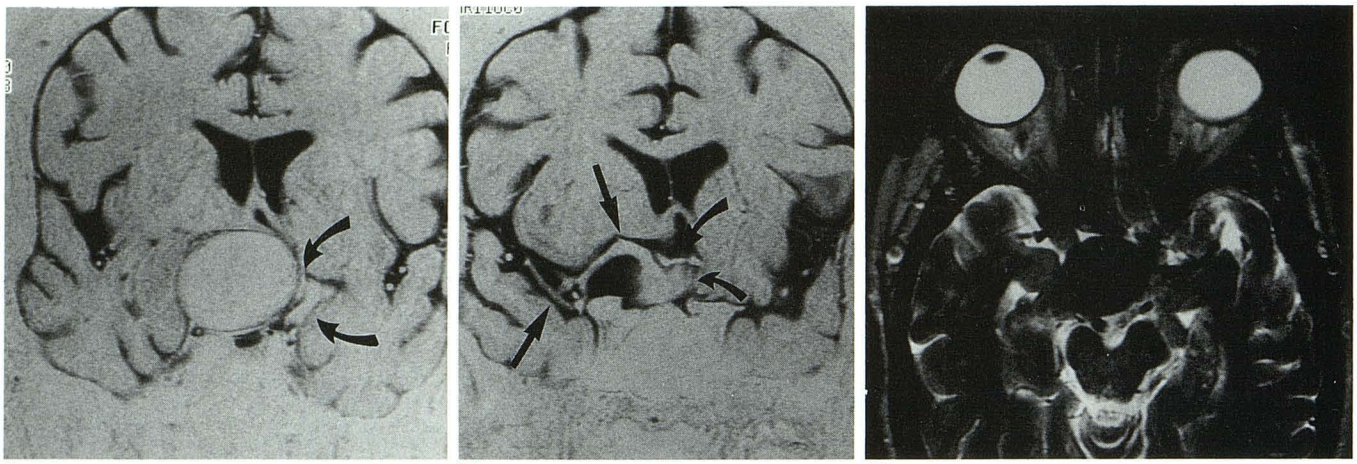

Fig 5. Giant supersellar aneurysm.

A, Coronal MR cisternography shows a well-defined round aneurysm displacing and compressing the optic chiasm (*upper arrow*). The medial border of the aneurysm extends close to left terminal internal carotid artery (*lower arrow*).

B, More-anterior coronal MR cisternography shows the normal positions of proximal anterior cerebral arteries (*upper curved arrow*). The medial border of the aneurysmal sac is shown by the *lower curved arrow*. Origin of the aneurysm is seen below the right carotid bifurcation (*upper straight arrow*). The normal right middle cerebral artery (*lower straight arrow*) is seen in a wide subarachnoid space because of upward displacement of the right basal ganglia.

C, Axial fast spin-echo (6500/108) shows the giant supersellar aneurysm.

pharyngioma showing proper location of the displaced normal optic chiasm that was not apparent on the conventional study. MR cisternography was also helpful in the evaluation of two cases with suprasellar aneurysms. The origin of a giant right internal carotid aneurysm could not be determined by catheter angiography because the very large sac covered all the segments of the carotid artery in various projections. MR cisternography determined the origin of the aneurysm below the carotid termination and above the cavernous sinus (Fig 5). In the second case, MR cisternography showed a moderate-size aneurysm arising by a wide neck from a diffusely ectatic distal carotid artery with dolichoectasia of both anterior and middle cerebral arteries. It was concluded that the aneurysm was inoperable, and catheter angiography was not performed.

There were two patients with orbital trauma. Conventional MR in both cases could not evaluate the suspected injuries of the optic nerves properly because of intraconal hemorrhage in one case and a granuloma scar in the other. MR cisternography depicted normal optic nerves through their entire courses in both cases (Fig 2) with the use of oblique sagittal composite MR cisternography images. Coronal MR cisternography, as well as conventional MR studies, failed to depict the normal optic nerves properly. Oblique sagittal composite MR cisternography is the procedure of choice for proper depiction of disease in relation to the optic nerves in the orbit.

Posterior Fossa

The posterior fossa cranial nerves were well depicted by the MR cisternography studies in this series. The fifth cranial nerve was clearly shown in appropriate sections, and in 50% of cases (n = 12 of 25) MR cisternography depicted vessels closely applied to the fifth nerves (Fig 6A). None of these patients had trigeminal neuralgia (9). Postoperative changes in the fifth nerve were revealed in two cases. In one case of trigeminal neuralgia, there was swelling of the fifth nerve after an isolation procedure. In the other case, postoperative MR cisternography showed residual acoustic neurinoma compressing and flattening the right fifth nerve. This finding was not seen on conventional MR.

In 25 cases in which sections were made through the petrous bones, the internal auditory subarachnoid recesses were outlined in 100% (n = 25). In only one case, an apparent defect was noted in the lateral portion of the left internal auditory subarachnoid recess on an individual section. A compressed image of three contiguous sections appeared normal.

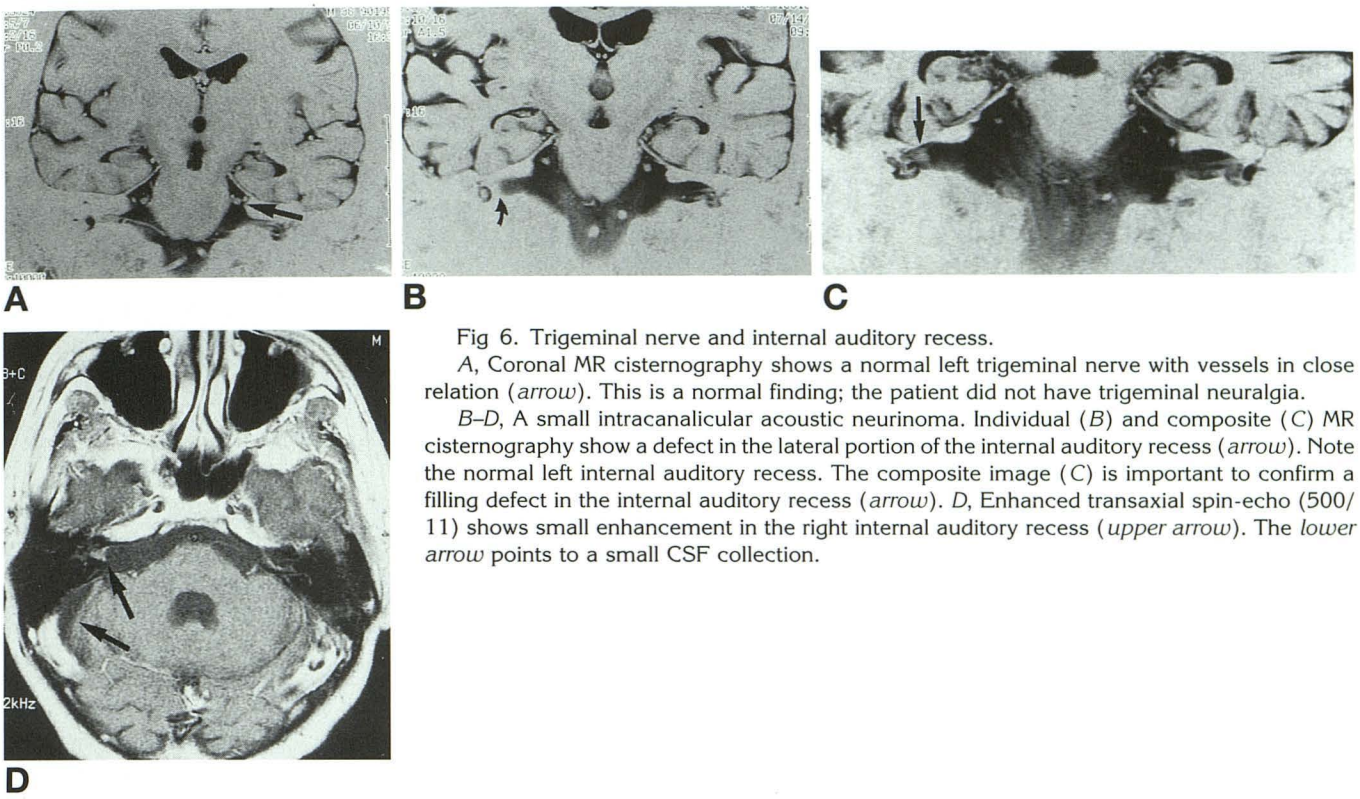

Fig 6. Trigeminal nerve and internal auditory recess.

A, Coronal MR cisternography shows a normal left trigeminal nerve with vessels in close relation (*arrow*). This is a normal finding; the patient did not have trigeminal neuralgia.

B–D, A small intracanalicular acoustic neurinoma. Individual (*B*) and composite (*C*) MR cisternography show a defect in the lateral portion of the internal auditory recess (*arrow*). Note the normal left internal auditory recess. The composite image (*C*) is important to confirm a filling defect in the internal auditory recess (*arrow*). *D*, Enhanced transaxial spin-echo (500/11) shows small enhancement in the right internal auditory recess (*upper arrow*). The *lower arrow* points to a small CSF collection.

Compressed-image MR cisternography is essential in the evaluation of intracanalicular masses. In a case of small acoustic neurinoma examined by MR cisternography a small defect was noted on the individual section and was also seen on the composite MR cisternography image. The corresponding conventional MR study showed a mildly enhancing lesion (Fig 6B–D). It is possible to use MR cisternography in the evaluation of intracanalicular lesions without the use of gadolinium enhancement, which is cost effective and also reduces scanning time. The internal jugular recess has a variable appearance. It may appear oblong, similar to the internal auditory recess, but also can have a globular or linear appearance. The lower cranial nerves were clearly depicted by MR cisternography.

As in the suprasellar region, MR cisternography delineates the outer surface of the posterior fossa vessels, providing an extraluminal angiogram. In one case of giant basilar artery aneurysm, MR cisternography provided valuable preoperative information (Fig 7). In addition to the basilar aneurysm, this series included two meningiomas presenting as posterior fossa masses. In one case of falx meningioma, conventional enhanced MR showed a thick enhancing right tentorial leaflet, a "dural tail," which could have been caused by either en plaque tumor or nonneoplastic reactive change (10, 11). MR cisternography showed the right tentorium to be of normal thickness. This was useful preoperative information, consistent with absence of tumor extension in the tentorium. Dural thickening seen on MR cisternography probably represents true pathologic change. One of our atrophy cases also had healed intracranial sarcoidosis, and MR cisternography depicted a thickened tentorial leaflet caused by healed granuloma. In another case of posterior fossa meningioma, the extraaxial location of the tumor was shown on MR cisternography with a layer of CSF separating the meningioma from the cerebellum.

Cerebral Hemispheres and Ventricles

MR cisternography showed in great detail the surface brain gyri and important sulci. Cortical veins were easily depicted as they coursed in the adjacent CSF on the coronal sections. Depiction of normal cortical veins on conventional MR sagittal views was reported to be a helpful sign in the differentiation between focal wide subarachnoid space and chronic subdural fluid

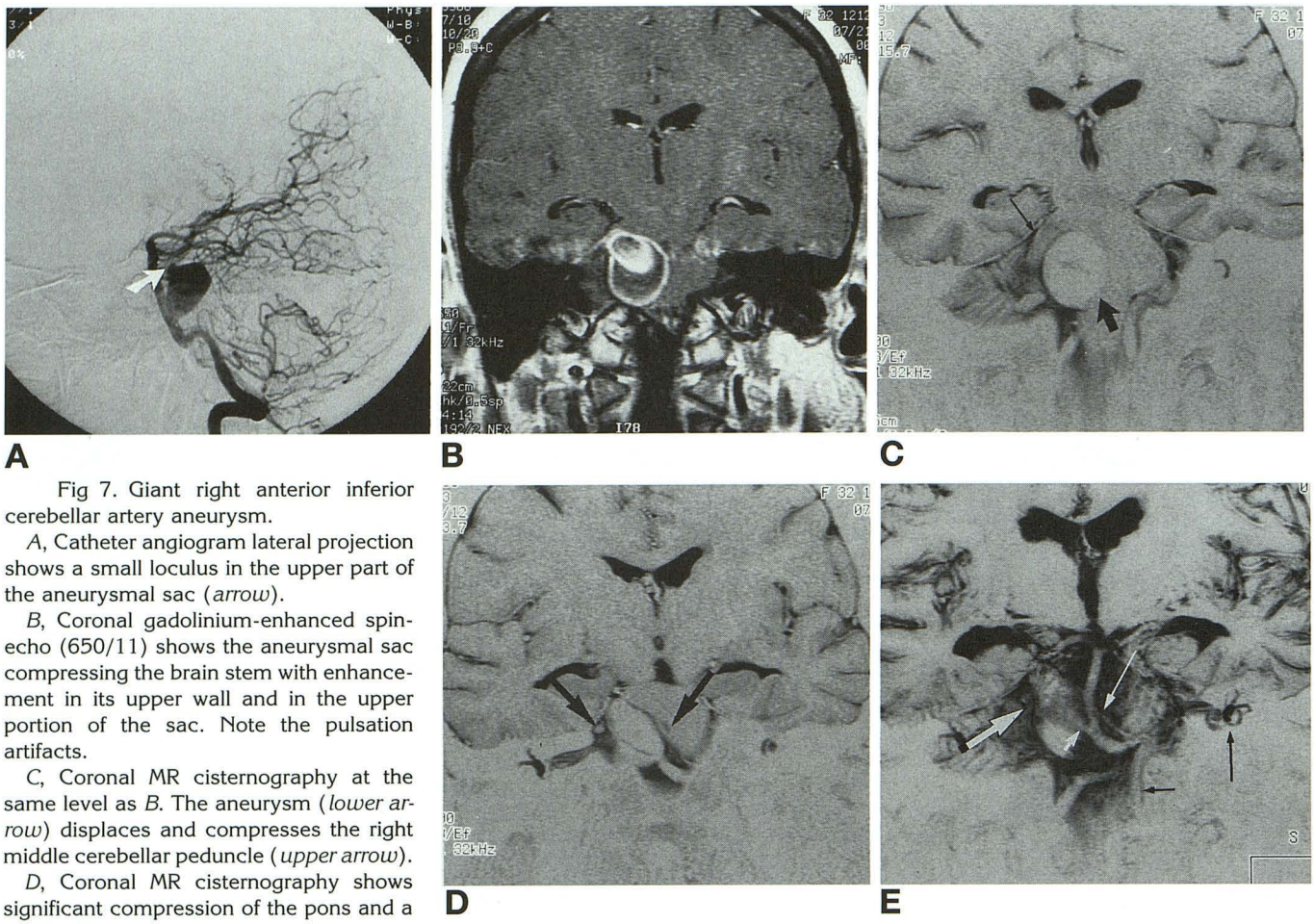

Fig 7. Giant right anterior inferior cerebellar artery aneurysm.

A, Catheter angiogram lateral projection shows a small loculus in the upper part of the aneurysmal sac (*arrow*).

B, Coronal gadolinium-enhanced spin-echo (650/11) shows the aneurysmal sac compressing the brain stem with enhancement in its upper wall and in the upper portion of the sac. Note the pulsation artifacts.

C, Coronal MR cisternography at the same level as *B*. The aneurysm (*lower arrow*) displaces and compresses the right middle cerebellar peduncle (*upper arrow*).

D, Coronal MR cisternography shows significant compression of the pons and a small infarct (not seen on the conventional MR study) (*left arrow*). The fifth nerve is seen lateral to the aneurysmal sac (*right arrow*).

E, Composite coronal image MR cisternography shows the neck of the aneurysm from the basilar artery close to right anterior inferior cerebellar artery (*small right arrow*). The left anterior inferior cerebellar artery is shown by the *left upper arrow*. Left inner ear structures (semicircular canals, cochlea, and vestibule) are depicted by the *left middle arrow*, and the left vertebral artery is shown by the *left lower arrow*. The *large right arrow* points to the origin of the upper loculus of the aneurysm, which was better depicted on sagittal MR cisternography (not shown).

accumulation (12). However, we had two cases of subdural hygroma in which straight cortical veins were apparent coursing through the fluid separating the brain from the inner table shown on conventional sagittal MR studies. We believe that coronal MR cisternography is more reliable in the diagnosis of "cortical vein sign," helping to differentiate a wide subarachnoid space from subdural fluid accumulation.

MR cisternography with suppression of the brain parenchyma signal better depicts the ventricles and their contours. MR cisternography should be able to show small changes in relation to the foramina of Monro. MR cisternography more effectively depicts small areas of brain disease having increased water content in close proximity to the ventricles as was seen in three cases in this series (n = 3 of 41) and also near the brain surface (n = 1 of 41) (Fig 7D). The aqueduct could not be clearly depicted by MR cisternography because of the increased CSF pulsatile flow within the aqueduct.

MR cisternography was valuable in the differentiation of intraaxial and extraaxial lesions in three patients in this series. These included a patient with a suprasellar tumor blocking the foramen of Monro and involving both frontal lobes with calcification and cyst formation. MR cisternography was helpful in showing the intraaxial location of the tumor before surgery. Conventional MR findings were inconclusive in this case. In another patient with multiple intra-

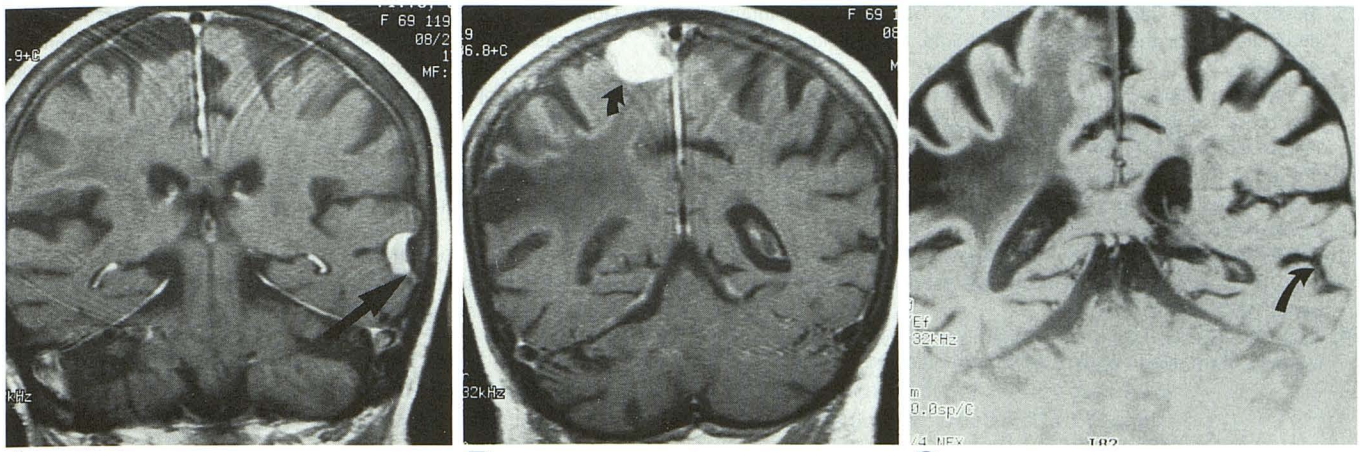

Fig 8. MR cisternography determines intraaxial versus extraaxial location of masses in a patient with renal cell carcinoma.

A and *B*, Gadolinium-enhanced coronal spin-echo (650/11) images; in *A*, a small enhancing mass in the left posterior hemicranium associated with hyperostosis (*arrow*) suggests the diagnosis of meningioma. *B*, Another mass noted in the right parasagittal parietal region (*arrow*). The location was indeterminate by conventional MR; another meningioma could not be excluded.

C and *D*, Coronal MR cisternography. The left meningioma (*C*) is seen surrounded by CSF separating it from the indented brain (*arrow*). The parasagittal lesion on the right (*D*) is seen as an intracerebral mass by MR cisternography (*arrow*). The high signal (reversed video) in the right hemisphere below the mass represents an old infarct.

cranial tumors with renal cell carcinoma (Fig 8), the determination of the intraaxial location of a high parasagittal lesion as determined by MR cisternography averted unnecessary catheter angiography or surgical biopsy in the treatment of the patient. MR cisternography was also able to determine the correct extraaxial location of a posterior fossa meningioma.

In conclusion, the accurate and noninvasive delineation of fistulous tracks by MR cisternography now makes it the procedure of choice in the evaluation of patients with suspected cranial CSF fistulas. MR cisternography provides important additional preoperative and postoperative information in patients with intracranial masses projecting into the subarachnoid space in the suprasellar region and in the posterior fossa. Depiction of small intracanalicular masses by MR cisternography in patients with suspected acoustic neurinoma provides a cost-effective alternative to conventional MR with gadolinium enhancement. Composite sagittal oblique MR cisternography images also proved excellent in the delineation of the entire course of the optic nerve and are recommended when additional or more detailed evaluation is indicated for patients with orbital disease.

References

1. Roberson J, Brismar J, Davis K, et al. Metrizamide cisternography with hypocycloidal tomography: preliminary results. *AJR Am J Roentgenol* 1976;127:965–967
2. El Gammal T. Cervical myelography and posterior fossa examinations with amipaque: use of magnification and subtraction. *Radiology* 1980;136:219–222
3. El Gammal T, Brooks BS. Serial biplane magnification and subtraction myelocisternography: normal and pathological findings. *AJNR Am J Neuroradiol* 1981;2:55–63
4. El Gammal T, Brooks BS. Myelography in the evaluation of the craniovertebral junction. In: Taveras M, Ferrucci JT Jr, eds. *Radiology: Diagnosis/Imaging/Intervention.* Philadelphia: Lippincott, 1986:1–7

5. Massey CE, El Gammal T, Brooks BS. Giant posterior inferior cerebellar artery aneurysm with dysphagia. *Surg Neurol* 1984;22: 467–471
6. Drayer BP, Wilkins RH, Boehnke M, Horton JA, Rosenbaum AE. Cerebrospinal fluid rhinorrhea demonstrated by metrizamide CT cisternography. *AJR Am J Roentgenol* 1977;129:149–151
7. Mawad M, Silver A, Hilal S, Ganti S. Computed tomography of the brainstem with intrathecal metrizamide, I: the normal brain stem. *AJNR Am J Neuroradiol* 1983;4:1–11
8. Krudy AG. MR myelography using heavily T2 weighted fast spin-echo pulse sequences with fat presaturation. *AJR Am J Roentgenol* 1992:159:1315–1320
9. Tash RR, Sze G, Leslie DR. Trigeminal neuralgia: MR imaging features. *Radiology* 1989;172:767–770
10. Goldsher D, Litt AW, Pinto RS, Bannon KR, Kricheff II. Dural "tail" associated with meningiomas on Gd-DTPA-enhanced MR images: characteristics, differential diagnostic value, and possible implication for treatment. *Radiology* 1990;176: 447–450
11. Tokumaru A, O'uchi T, Eguchi T, et al. Prominent meningeal enhancements adjacent to meningioma on Gd-DTPA-enhanced MR images: histopathologic correlation. *Radiology* 1990;175: 431–433
12. McCluney KW, Yeakley JW, Fenstermacher JM, Baird SH, Bonmati CM. Subdural hygroma versus atrophy on MR brain scans. *AJNR Am J Neuroradiol* 1992;13:1335–1339.